CrossMark

research paper

Check for updates

Acta Cryst D STRUCTURAL BIOLOGY

ISSN 2059-7983

The cap-binding site of influenza virus protein PB2 as a drug target

Chelsea Severin,[a] Tales Rocha de Moura,[a] Yong Liu,[b] Keqin Li,[a] Xiaofeng Zheng[b]* and Ming Luo[a]*

[a]Department of Chemistry, Georgia State University, PO Box 3965, Atlanta, GA 30302, USA, and [b]State Key Laboratory of Protein and Plant Gene Research and School of Life Sciences, Peking University, Beijing 100871, People's Republic of China. *Correspondence e-mail: xiaofengz@pku.edu.cn, mluo@gsu.edu

Received 27 October 2015
Accepted 3 January 2016

Edited by R. McKenna, University of Florida, USA

Keywords: antiviral; inhibitor; drug design; broad spectrum.

PDB references: CA09-PB2cap, 5eg9; mutant CA09-PB2cap, 5eg8; mutant CA09-PB2cap, complex with m^7GTP, 5eg7

Supporting information: this article has supporting information at journals.iucr.org/d

The RNA polymerase of influenza virus consists of three subunits: PA, PB1 and PB2. It uses a unique 'cap-snatching' mechanism for the transcription of viral mRNAs. The cap-binding domain of the PB2 subunit (PB2cap) in the viral polymerase binds the cap of a host pre-mRNA molecule, while the endonuclease of the PA subunit cleaves the RNA 10–13 nucleotides downstream from the cap. The capped RNA fragment is then used as the primer for viral mRNA transcription. The structure of PB2cap from influenza virus H1N1 A/California/07/2009 and of its complex with the cap analog m^7GTP were solved at high resolution. Structural changes are observed in the cap-binding site of this new pandemic influenza virus strain, especially the hydrophobic interactions between the ligand and the target protein. m^7GTP binds deeper in the pocket than some other virus strains, much deeper than the host cap-binding proteins. Analysis of the new H1N1 structures and comparisons with other structures provide new insights into the design of small-molecule inhibitors that will be effective against multiple strains of both type A and type B influenza viruses.

1. Introduction

Influenza virus causes seasonal epidemics that affect the health of millions of people every year (Klepser, 2014). Occasionally, a new pandemic strain emerges that can circulate the world in a short period of time, such as the pandemic strain of H1N1 influenza A virus in 2009 (pH1N1 2009; Fraser *et al.*, 2009). Since influenza virus mutates rapidly and new strains emerge frequently through the reassortment of viral strains originating from different hosts, new pandemic strains are expected. Control of influenza virus is therefore a major public health task. In addition to vaccines, antiviral drugs are a cost-effective means of controlling the spread of the virus. These drugs usually have a broad spectrum of activities against multiple influenza virus strains and can be stored on a relatively long term in strategic sites for rapid responses when new virus strains emerge. However, resistant strains of influenza virus have regularly been identified (Nitsch-Osuch & Brydak, 2014). Frequently prescribed anti-influenza drugs such as oseltamivir and zanamivir that are on the market today primarily target one viral protein: influenza virus neuraminidase. Furthermore, the Centers for Disease Control and Protection (CDC) report that high levels of resistance to the adamantanes (amantadine and rimantadine) persist among the influenza A viruses currently circulating. Adamatanes are ineffective against influenza B viruses. Consequently, it is desirable to have a panel of antiviral drugs that target other viral proteins.

Influenza virus has a unique mechanism for its viral transcription (Ruigrok *et al.*, 2010). The viral RNA-dependent

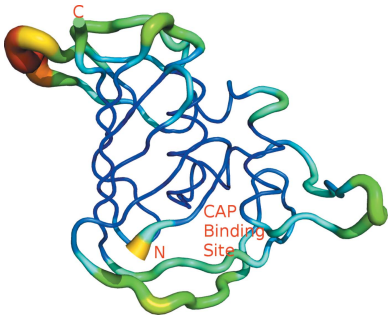

RNA polymerase (vRdRp) of influenza virus has three virus-encoded subunits: PA, PB1 and PB2. The vRdRp does not synthesize the cap of viral mRNAs; instead, it uses a primer-dependent mechanism for stealing a cap from the host pre-mRNA. The PB2 cap-binding domain (PB2cap) is responsible for binding the 5′-cap on host pre-mRNAs; the PA endonuclease then cleaves the snatched pre-mRNA 10–13 nucleotides downstream of the cap. The resulting oligonucleotide is used as a primer to initiate polymerization by the PB1 subunit. The crystal structure and functions of PB2cap have been carefully studied (Tarendeau *et al.*, 2007; Liu *et al.*, 2013; Tsurumura *et al.*, 2013). The m^{7}GTP binding site consists of a hydrophobic side chain (residue His357 in influenza A virus or Trp359 in influenza B virus) and a cluster of four aromatic residues (Fig. 1*a*). The purine moiety is sandwiched between the two hydrophobic side chains (His357 and Phe404). In addition, two hydrogen bonds are formed by the purine moiety to the side chains of Glu361 and Lys376, respectively. The ribose and the triphosphate may interact with PB2cap as well, but their contribution to m^{7}GTP binding appears to be less critical (Liu *et al.*, 2013). It has been shown that the structure of PB2cap is different from the cap-binding domains of other proteins, including human proteins, and that the cap-binding site of PB2cap is conserved among different strains of influenza virus (Guilligay *et al.*, 2008). For instance, the cap moiety is sandwiched between a His residue and a cluster of hydrophobic residues (Phe) in a deep pocket in PB2cap of influenza A virus. In the human cap-binding protein, however, it is sandwiched between two Tyr residues and its phosphate moiety is buried inside the binding site. PB2cap is therefore a viable target for broad-spectrum antiviral agents against influenza virus (Pautus *et al.*, 2013).

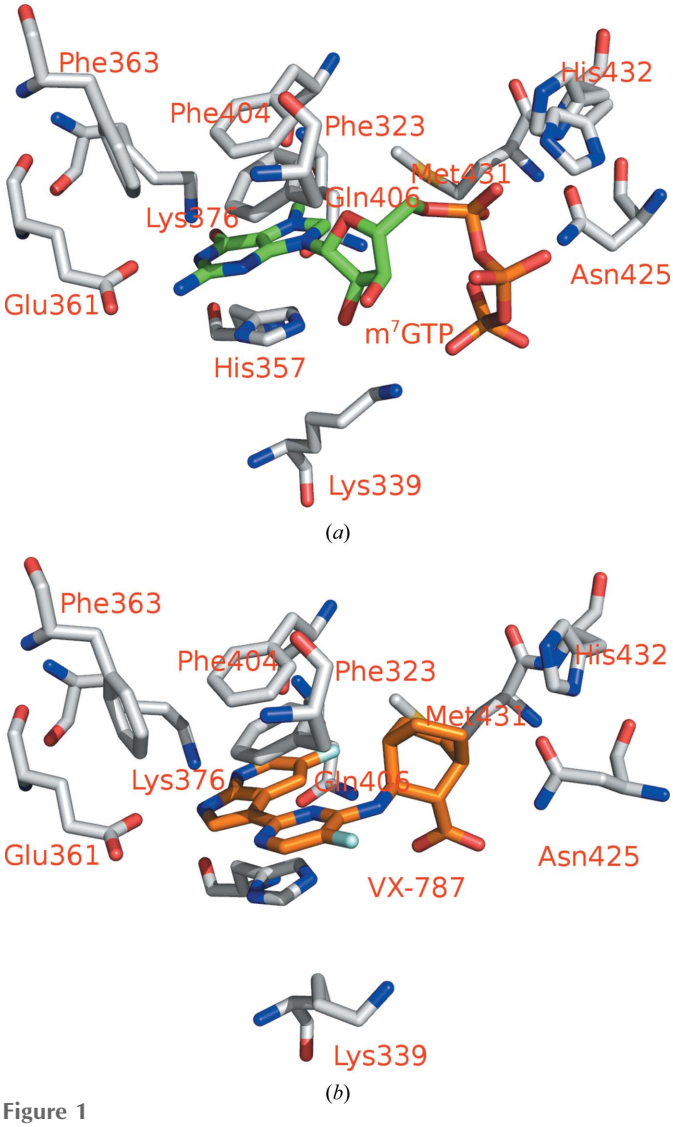

Figure 1
The cap-binding site in PB2cap: (*a*) A/California/07/2009 PB2cap bound to m^{7}GTP (PDB entry 5eg7), (*b*) A/Victoria/3/1975 PB2cap bound to VX-787 (PDB entry 4p1u; Clark *et al.*, 2014). The residues are labeled according to the numbering of A/California/07/2009 PB2cap in this and the following figures. Each ligand in the PB2cap binding site is also labeled.

The structures of inhibitors in complex with PB2cap have previously been reported (Pautus *et al.*, 2013; Clark *et al.*, 2014). A series of m^{7}GTP derivatives have been synthesized with modifications at the N-2, N-7 and N-9 positions of the guanine moiety (Pautus *et al.*, 2013). The compounds that showed good activities in blocking m^{7}GTP binding mostly have a methyl group at the N-7 position, indicating a limited space for accommodating large groups at this position. The main modification that yielded good inhibitory activities is at the N-9 position, where an aromatic moiety was added to replace the pyranose in the cap structure. This aromatic moiety shows hydrophobic interactions with the side chain of Phe323 (Pautus *et al.*, 2013). Recently, a new structure showed that a cyclohexyl carboxylic acid analogue (named VX-787) binds in the cap-binding site with the azaindole moiety replacing the 7-methylguanidine (Fig. 1*b*). The azaindole moiety recapitulates both the hydrophobic interactions and hydrogen bonds of the purine moiety in the cap. In addition, the cyclohexyl carboxylic group is coupled to azaindole *via* fluoropyrimidine. The cyclohexyl group provides more hydrophobic interactions with the cluster of four aromatic residues. The carboxyl group may form hydrogen bonds to two ordered water molecules. VX-787 reportedly has a strong potency to inhibit a number of influenza A virus strains (Clark *et al.*, 2014), but showed negligible activity against influenza B virus (Byrn *et al.*, 2015). To explore the potential of designing a potent inhibitor that is effective against multiple strains of both type A and type B influenza viruses, we solved the crystal structures of PB2cap from pH1N1 A/California/07/2009 and its complex with m^{7}GTP at resolutions of 1.54 and 1.40 Å, respectively. By comparing with different structures, we show that the cap-binding site has a measurable flexibility to accommodate a compound that fits in the hydrophobic pocket. The hydrogen bonds to the side chains of Glu361 and Lys376 should be established because the inhibitor needs to displace a few ordered water molecules that interact with these side chains. It is also necessary to establish a hydrogen bond to the side chain of Arg334 in influenza B virus (Arg332 in influenza A virus) if the same inhibitor is to also bind influenza B virus PB2cap (Liu *et al.*, 2015).

2. Materials and methods

2.1. Protein expression and purification

The DNA coding sequence for PB2cap from A/California/07/2009 H1N1 (CA09-PB2cap) was inserted into pET-28a vector between NdeI and XhoI sites to generate a His_6-tag fusion protein with a thrombin cleavage site. Protein expression was carried out in *Escherichia coli* BL21 (DE3) cells and expression was induced with 0.5 m*M* isopropyl β-D-1-thiogalactopyranoside (IPTG) at 18°C for 18 h. The recombinant protein was purified using a nickel-affinity column (Ni^{2+}-charged HiTrap chelating HP column from GE Healthcare). The His_6 tag was removed by incubation with thrombin protease for 4 h at 25°C and the sample was applied onto an Ni^{2+}-charged HiTrap column again to remove uncleaved protein. The protein was further purified by gel-filtration chromatography using a Superdex 75 column (GE Healthcare) previously equilibrated with 10 m*M* Tris pH 8.0, 200 m*M* NaCl. The fractions corresponding to the PB2cap protein were pooled and concentrated to 4–10 mg ml^{-1} for crystallization. The expression vector for the PB2cap truncation mutant was generated using a QuikChange kit (Agilent Technologies, California, USA) and the protein was purified following the same procedure as used for native PB2cap.

Table 1
Data-collection and refinement statistics.

Values in parentheses are for the highest resolution shell.

Protein	CA09-PB2cap	m^7GTP–mutant CA09-PB2cap	Mutant CA09-PB2cap
PDB code	5eg8	5eg7	5eg9
Data collection			
Space group	$P3_121$	$P4_32_12$	$P12_11$
Unit-cell parameters			
a (Å)	54.61	45.26	37.13
b (Å)	54.61	45.26	109.01
c (Å)	196.49	156.40	39.66
α (°)	90	90	90
β (°)	90	90	90.54
γ (°)	120	90	90
Molecules in asymmetric unit	2	1	2
Wavelength (Å)	0.9795	1.0000	1.0000
Resolution (Å)	15–1.54 (1.59–1.54)	25–1.40 (1.42–1.40)	50–2.30 (2.34–2.30)
R_{merge}† (%)	7.0 (21.4)	7.1 (61.1)	7.1 (19.4)
$\langle I/\sigma(I)\rangle$	57.9 (14.2)	33.2 (1.8)	21.2 (6.2)
$CC_{1/2}$	0.997 (0.992)	0.912 (0.581)	0.893 (0.906)
Completeness (%)	97.2 (96.9)	99.8 (97.0)	87.7 (92.6)
Multiplicity	15.1 (16.7)	10.4 (4.0)	1.8 (1.7)
Refinement			
Resolution (Å)	14.63–1.54	25–1.40	19.83–2.30
No. of reflections	47547	31406	11663
R_{work}/R_{free}‡ (%)	12.2/17.7	12.4/16.9	19.0/25.6
Average *B* factor (Å^2)	24.9	16.1	29.3
R.m.s. deviations			
Bond lengths (Å)	0.019	0.020	0.014
Bond angles (°)	1.93	2.35	1.65
Ramachandran plot (%)			
Favored region	97.5	98.1	96.8
Allowed region	2.2	1.9	2.6
Outlier region§	0.3	—	0.6

† $R_{merge} = \sum_{hkl}\sum_i |I_i(hkl) - \langle I(hkl)\rangle| / \sum_{hkl}\sum_i I_i(hkl)$. ‡ $R = \sum_{hkl} ||F_{obs}| - |F_{calc}|| / \sum_{hkl} |F_{obs}|$. R_{free} is calculated using 5% of the data, which were excluded from the refinement. § Outliers are in loop regions where no clear density was observed.

2.2. Crystallization and structure analyses

The native and mutant PB2cap proteins were subjected to crystal screens (Index, Natrix, PEG/Ion, Crystal Screen and Crystal Screen 2; Hampton Research, California, USA). After optimization, crystals were grown by vapor diffusion with a hanging drop consisting of 10 mg ml^{-1} native PB2cap protein mixed with a reservoir solution composed of 0.2 *M* magnesium nitrate 0.1 *M* HEPES pH 8.0, 20%(*w*/*v*) PEG 3350 and a hanging drop consisting of 4 mg ml^{-1} mutant PB2cap protein mixed with a reservoir solution composed of 0.1 *M* bis-tris pH 6.5, 15%(*w*/*v*) PEG 3350 at 20°C. Cocrystallization was carried out by adding 0.2 m*M* m^7GTP to the PB2cap solution and concentrating it to a final protein concentration of 4 mg ml^{-1}. The cocrystals were grown under the same condition as used for the protein without m^7GTP.

Protein crystals were transferred to a solution of mother liquor containing 20% glycerol and were flash-cooled in liquid nitrogen. X-ray diffraction data were collected at Shanghai Synchrotron Radiation Facility, China and SER-CAT at the Advanced Photon Source, USA. Data processing was carried out with the *HKL*-2000 program suite. Molecular replacement was performed with *MOLREP* using the coordinates of PDB entry 4enf (Liu *et al.*, 2013) as the search model. The structure of the mutant PB2cap was solved with the native structure following the same protocol. Structural refinement was carried out with *REFMAC*5. *MOLREP* and *REFMAC*5 are part of the *CCP*4 crystallographic package (Winn *et al.*, 2011). X-ray crystallographic analyses are summarized in Table 1. The coordinates of the reported structures were downloaded from the RCSB PDB. Structure superposition and figure preparation were carried out using *PyMOL* (v.1.3; Schrödinger).

3. Results and discussion

3.1. The cap-binding site in PB2 of A/California/07/2009

The deeper end of the cap-binding site contains two critical residues: Glu361 and Lys376. The side chains of these two residues form hydrogen bonds to the guanine moiety when the cap binds. The side chain of Glu361 has a stable conformation, whereas that of Lys376 may assume two different conformations (Fig. 2*a*), one of which is suitable for forming the hydrogen bond to the guanine moiety. There are also two important residues with aromatic side chains: His357 and

Phe404. These side chains sandwich the guanine moiety by π–π stacking interactions. The side chain of His357 appears to rotate when the cap-binding site is empty (Fig. 2*b*). The orientation of the His357 side chain is different in A/California/07/2009 (H1N1) PB2cap compared with that in A/PR/8/34 (H1N1) PB2cap (Fig. 2*b*). Next, the side chain of Phe323 makes hydrophobic interactions with the pyranose in the cap. Moreover, the side chain of Lys339 is in a position to form a hydrogen bond to the 2′-OH of the pyranose, but it rotates away when the cap-binding site is empty. Further out, the side chain of His432 may be involved in charge interactions with the α-phosphate group in the cap, but its orientation is quite flexible. The side chain of Asn429 is also in position to form a hydrogen bond to the α-phosphate group, but it shows two orientations when the cap-binding site is empty.

There is an ordered water molecule that forms a hydrogen bond to the carbonyl group of Phe404 (Fig. 2*a*). This water molecule is displaced when the cap binds. A thiocyanate group from the crystallization solution is modeled in a pocket lined by the side chains of Gln406 and Met431. In the structure of A/PR/8/34 PB2cap, a nitrate group from the crystallization buffer is modeled in a nearby position. These observations suggest that there is a large space at this location.

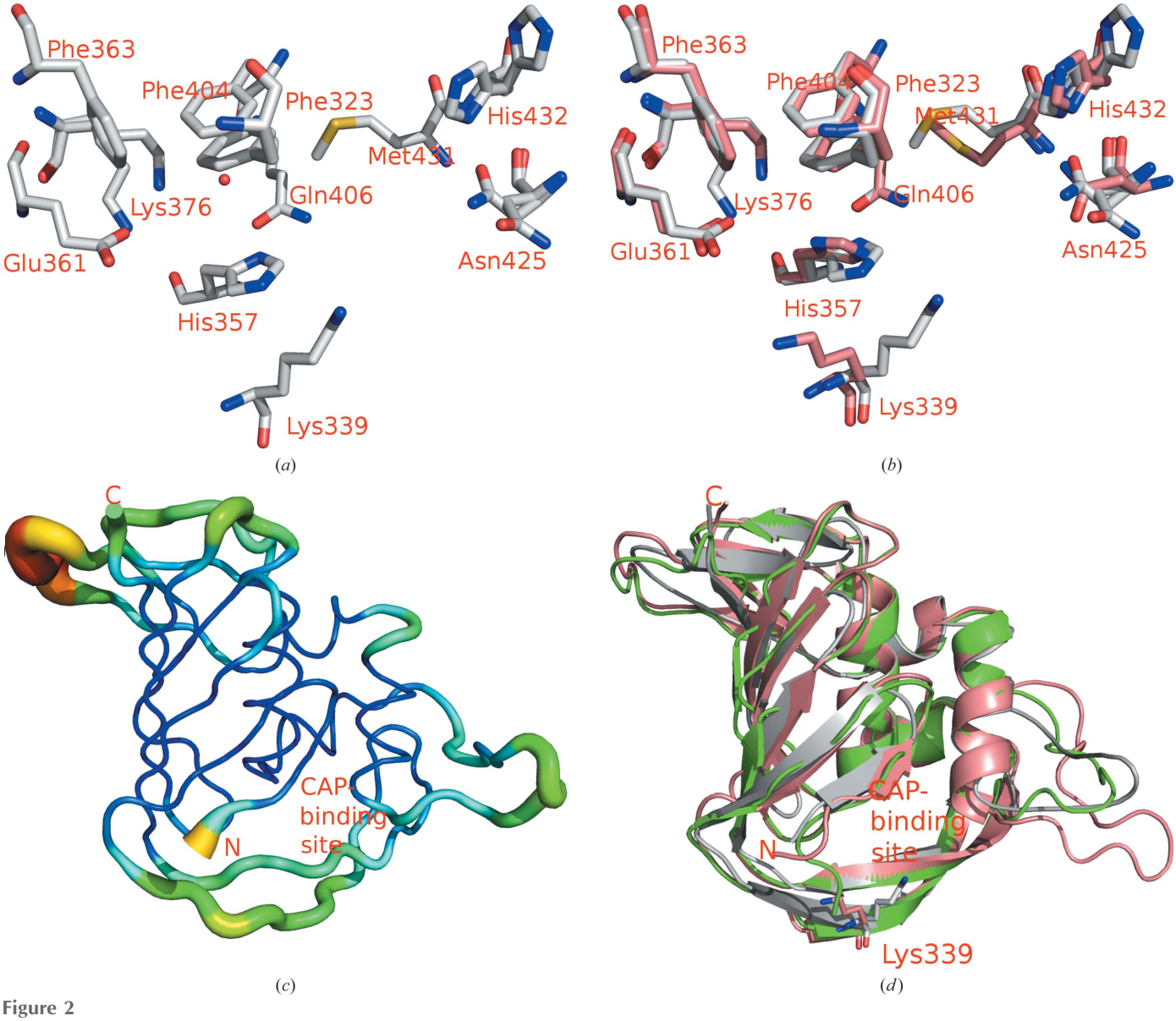

Figure 2
(*a*) The cap-binding site in PB2cap of A/California/07/2009 (PDB entry 5eg8); 11 residues (labeled) and one water molecule (sphere) are shown. Lys376, Asn429 and His432 are represented by two alternative side-chain conformations. (*b*) Comparisons of the cap-binding site in A/California/07/2009 PB2cap (gray) and A/PR/8/34 PB2cap (PDB entry 4enf; pink; Liu *et al.*, 2013). Residues Lys376, Asn429 and His432 in A/PR/8/34 PB2cap do not show alternative conformations. (*c*) A main-chain diagram of A/California/07/2009 PB2cap; the *B* factor is used to puff the trace (*PyMOL*). The N- and C-termini are labeled N and C, respectively. The location of the cap-binding site is indicated. (*d*) Comparison of three PB2cap structures: native (gray), mutant (green) and A/PR/8/34 (pink); residue Lys339 is labeled. The N- and C-termini are labeled N and C, respectively. The location of the cap-binding site is indicated.

The most flexible regions are located in the large loops (Fig. 2*c*). However, the main-chain conformation near the cap-binding site also showed some flexibility. The major differences are in the region from Thr333 to Lys339 and the region from Ala413 to Lys440 (Fig. 2*d*). Thr333 is at the end of a β-strand and the polypeptide makes a sharp turn into the next β-strand ending at Lys340. In A/PR/8/34 PB2cap, this region opens more widely so that the side chain of Lys339 is no longer in a position to interact with the cap. Ala413 is at the start of an α-helix, followed by a large flexible loop that ends at Lys440. This loop has a large influence in crystallization. In the native PB2cap of A/California/07/2009 the side chain of Arg423 in the loop occupies the cap-binding site, bridging strong interactions between two molecules in the asymmetric unit. Attempts to soak m^{7}GTP into the crystal or to cocrystallize with PB2cap of A/California/07/2009 both failed. Since the Arg432 loop blocks the cap-binding site, we therefore replaced residues Val421–Arg427 with a GSG linker to cut the loop short. The shortened loop resulted in the loss of one turn in the α-helix. On the other hand, this helix has one extra turn in the PB2cap of A/PR/8/34, leading to a different conformation of the following loop. Overall, the cap-binding site in PB2cap showed considerable flexibility observed as alternative side-chain orientations of the active-site residues and an alternative conformation of the secondary-structure elements near the cap-binding site. These factors should be taken into account when an inhibitor is designed to tightly bind the active site in PB2cap of all influenza virus strains.

3.2. Interactions between m^{7}GTP and the cap-binding site

As mentioned above, efforts to soak m^{7}GTP into the crystal of the native PB2cap of A/California/07/2009 were unsuccessful. When cocrystallization was attempted, the crystals obtained did not contain m^{7}GTP. We therefore carried out mutagenesis to shorten the loop that occupies the cap-binding site of the neighboring molecule in the asymmetric unit. The mutant PB2cap was subjected to crystal screens, and protein crystals were grown using 0.1 *M* bis-tris pH 6.5, 15%(*w*/*v*) PEG 3350 as the reservoir solution. However, the crystals dissolved when soaked in mother liquor containing 1 m*M* m^{7}GTP, indicating that a large conformational change was induced by cap binding. Cocrystals of m^{7}GTP were grown with the mutant PB2cap using the same reservoir solution. Comparisons between the native and the complex structures revealed the conformational changes when m^{7}GTP binds to the cap-binding site (Fig. 3*a*). All structures used in the comparisons have been determined at 1.5 Å resolution or better. The truncated mutant PB2cap has essentially the same structure as the native PB2cap (r.m.s.d. of 0.379 Å for 905 aligned atoms), except that the side chain of His357 has a

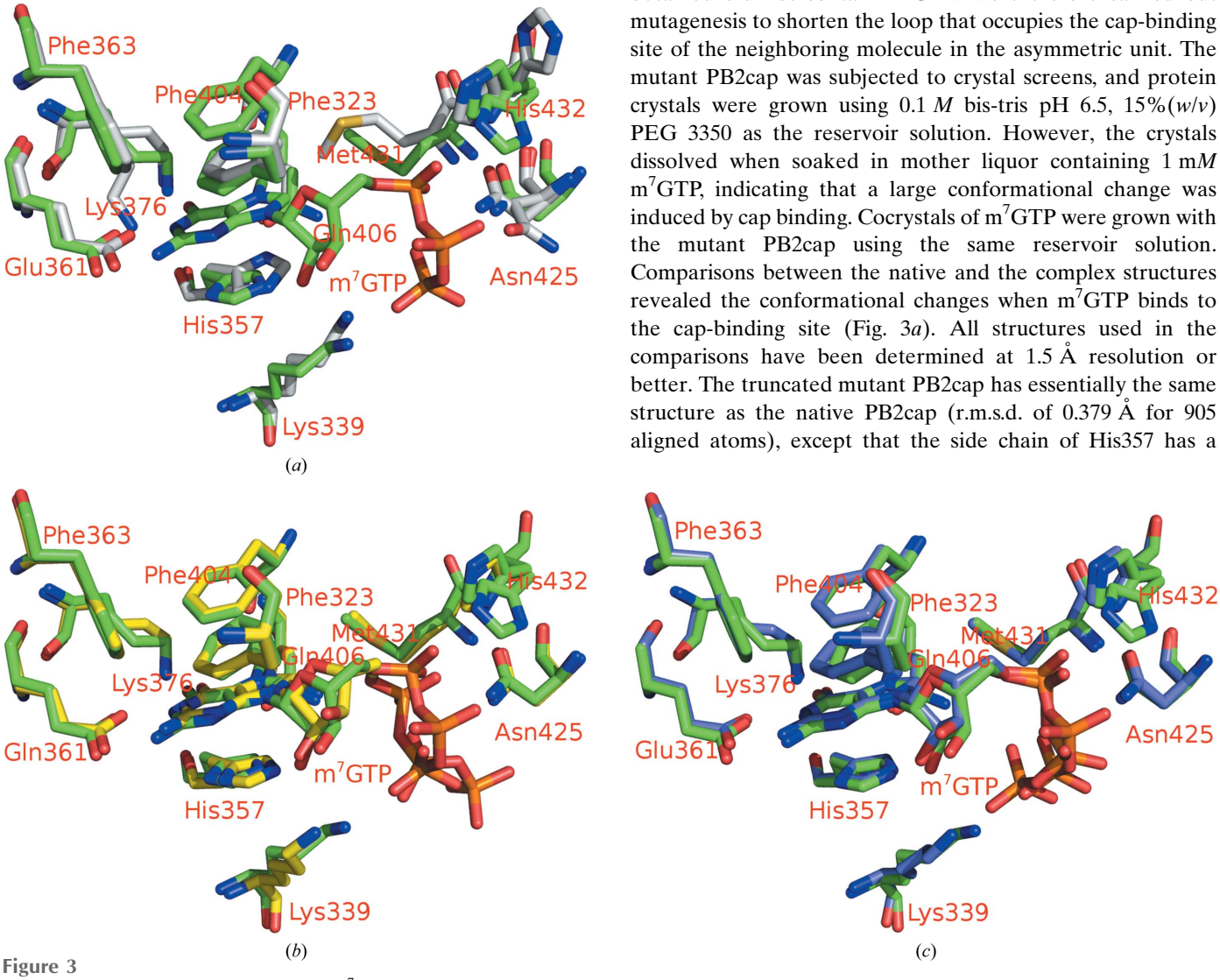

Figure 3
(*a*) Comparison of the native (gray) and m^{7}GTP-bound (green) cap-binding site in A/California/07/2009 PB2cap. Lys376 and Asn425 showed only one conformation in the complex, whereas His357, Met431 and His432 have alternative conformations in the complex. (*b*) Comparison of the cap-binding site with m^{7}GTP bound in A/California/07/2009 PB2cap (green) and A/Duck/Shantou/4610/2003 (H5N1) PB2cap (PDB entry 4cb4; yellow; Pautus *et al.*, 2013). These two structures have the closest superposition. (*c*) Comparison of the cap-binding site in m^{7}GTP-bound A/California/07/2009 PB2cap (green) and A/Hong Kong/1/68 PB2cap (H3N2; PDB entry 4eqk; blue; Liu *et al.*, 2013). The two structures are also superimpose well.

different orientation, indicating a very flexible conformation for this side chain. The truncated mutant PB2cap was not included in the comparisons.

In the complex of m^{7}GTP with the mutant PB2cap, it appears that the main chain around Glu361 has moved away by about 0.6 Å to allow the formation of proper hydrogen bonds between the side chain of Glu361 and the guanine moiety (Fig. 3*a*). The distances of the Glu361 carboxyl O atoms to N1 and NH2 at position 2 of the guanine moiety are now 2.7 and 2.9 Å, respectively. At the same time, the side chain of Lys376 assumed one conformation instead of the two possible conformations found in the native PB2cap in order to form a proper hydrogen bond to the carbonyl O atom at position 6. The ordered water molecule at the carbonyl group of Phe404 was clearly displaced. More visibly, the side chain of His357 was rotated so that it could make the most π–π stacking with the guanine moiety (Fig. 3*a*). The side chain of Phe404 is usually identified as contributing to π–π stacking on the other side of the guanine moiety (Guilligay *et al.*, 2008). However, the side chain of Phe323 is also in an appropriate position to form π–π stacking with the guanine moiety. Moreover, the side chain of Phe363 is within a suitable distance to make a T-shaped interaction with the guanine moiety. It is likely that the three aromatic side chains jointly make strong hydrophobic interactions with the guanine moiety. The methyl group at position 7 is located in a hydrophobic pocket formed by Phe404, Met431 and part of the Gln406 side chain. The side chain of Met431 actually retracted so that the distance between the two methyl groups changes from 3.0 Å (closest distance in van der Waals interactions) to 4.5 Å.

The 2′-OH group forms hydrogen bonds to the side chains of Lys339 and His357 in PB2cap of A/California/07/2009. The pyranose ring is roughly orthogonal to the guanine moiety. This ring may have some degree of hydrophobic interaction with the side chain of Phe323, but their orientation is not parallel and the distance is long. It may not make a significant contribution to cap binding. The α-phosphate group clearly makes salt-bridge and hydrogen-bond interactions with the side chains of His432 and Asn429. His432 assumes two conformations in the interactions, one of which overlaps with one of the two conformations in the native PB2cap. The Asn429 side chain assumes only one conformation that overlaps with one of the two conformations in the native PB2cap. The β-phosphate group could make a salt bridge with the side chain of Lys339, which moved from a distance of 2.2 to 2.7 Å. However, the conformation of the β-phosphate group as well as that of the γ-phosphate group change dramatically in different PB2cap structures. How the phosphate groups interact with PB2cap may only become clearer when the cap is placed in the context of the full-length viral polymerase complex. It is clear, however, that a positively charged residue, Lys or Arg, is conserved at position 339. Its side chain is highly likely to form a salt bridge to one of the phosphate groups in the cap.

The cap binding is also compared with PB2cap of A/Duck/Shantou/4610/2003 (H5N1; Pautus *et al.*, 2013; Fig. 3*b*) and A/Hong Kong/1/68 (H3N2; Liu *et al.*, 2013; Fig. 3*c*). In PB2cap of H5N1, m^{7}GTP is moved outwards from the cap-binding site by 0.5 Å. Accordingly, the side chain of His357 also moves to maintain the π–π stacking, accompanied by movement of the main chain. The pyranose ring is rotated by about 22.6° so that it has less inclination relative to the guanine moiety. As a result, the 2′-OH group no longer forms a hydrogen bond to the side chain of His357. The side chain of Lys339, on the other hand, still forms a hydrogen bond to the 2′-OH group, but it has to move towards the OH group accompanied by movement of the main chain. The conformation of all three phosphate groups is different in the three structures, and no consensus interactions may be discerned. In PB2cap of H3N2 all interactions are similar to those found in A/California/07/2009, except that the side chain of Phe323 is shifted owing

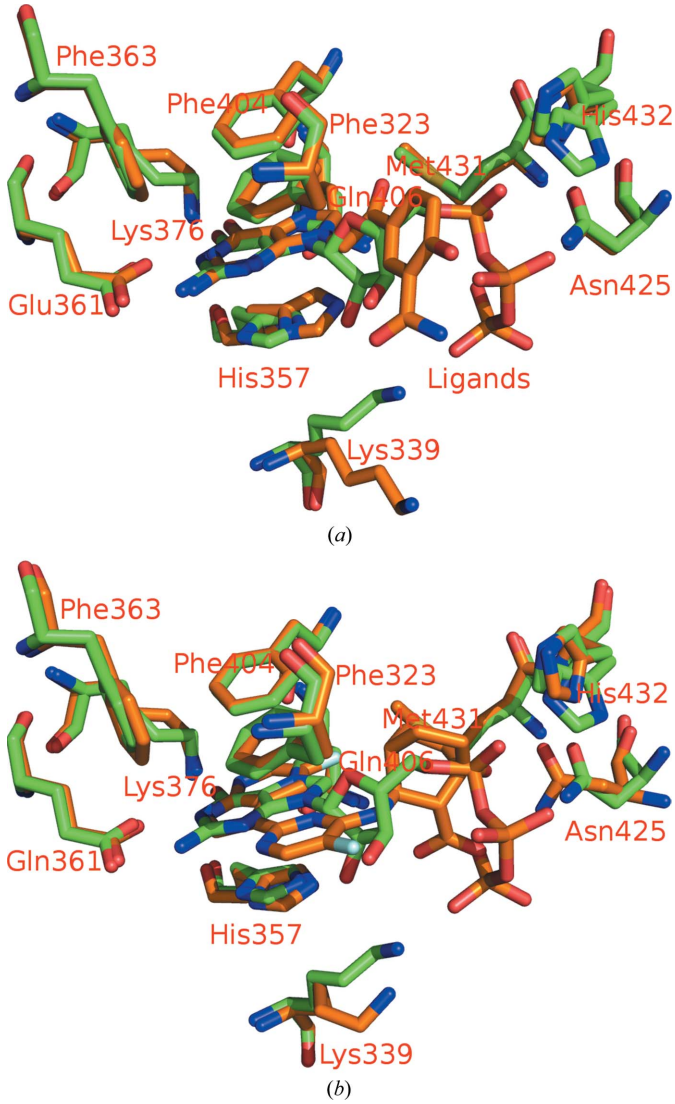

Figure 4
Comparison of the PB2cap cap-binding site. (*a*) A/California/07/2009 PB2cap bound to m^{7}GTP (green) and A/Duck/Shantou/4610/2003 PB2cap bound to compound **8f** (PDB entry 4cb5; orange; Pautus *et al.*, 2013). 'Ligands' indicate the locations of m^{7}GTP and **8f**. (*b*) A/California/07/2009 PB2cap bound to m^{7}GTP (green) and A/Victoria/3/1975 PB2cap bound to VX-787 (PDB entry 4p1u; orange; Clark *et al.*, 2014).

to movement of the main chain. Since Phe323 is close to the terminus of PB2cap, the crystal contacts may have an effect on its side-chain conformation.

3.3. Comparisons with PB2cap inhibitors

The structures of two classes of inhibitors in complex with PB2cap are available (Fig. 4). The complex of a representative compound (**8f**) with PB2cap of H5N1 A/duck/Shantou/4610/2003 PB2cap is used for comparison with the first class of inhibitors. Compound **8f** is a derivative of m^7-guanine and showed modest inhibition of cap binding to PB2cap (Pautus *et al.*, 2013). The structure shows that the guanine moiety of compound **8f** retains essentially the same interactions as those in m^7GTP (Fig. 4*a*). The phenyl group coupled to the guanine moiety should make some hydrophobic interactions with the side chain of Phe303, but is not close enough for π–π stacking. The hydroxyl group on the phenyl ring may form a hydrogen bond to the main chain *via* a water molecule. This compound has only limited interactions with PB2cap, consistent with its modest inhibitory activity.

On the other hand, the cyclohexyl carboxylic acid analogue VX-787 is a potent inhibitor (Clark *et al.*, 2014). In its complex with PB2cap of A/Victoria/3/1975 H3N2 (Fig. 4*b*), the N atom at position 4 of the azaindole moiety forms a hydrogen bond to the side chain of Glu361 and the N atom at position 9 forms a hydrogen bond to the side chain of Lys376. More importantly, the azaindole pyrimidinyl moiety is in a perfect position to make π–π stacking interactions with the side chains of Phe323 and Phe404 simultaneously. Furthermore, the bicyclooctane coupled to the pyrimidinyl moiety perfectly occupies the hydrophobic pocket formed by the side chains of Phe325 and Met431. Finally, the carboxyl group linked to the bicyclooctane forms a salt bridge with the side chain of Arg355 and hydrogen bonds to the side chains of His357 and Gln406 *via* water molecules. The side chain of Lys339 (Arg339) is close by. Its side chain could also form a salt bridge with the carboxyl group in different influenza A virus strains. VX-787 capitalizes on all available interactions with PB2cap and showed potent inhibitory activities against a number of influenza A virus strains (Clark *et al.*, 2014).

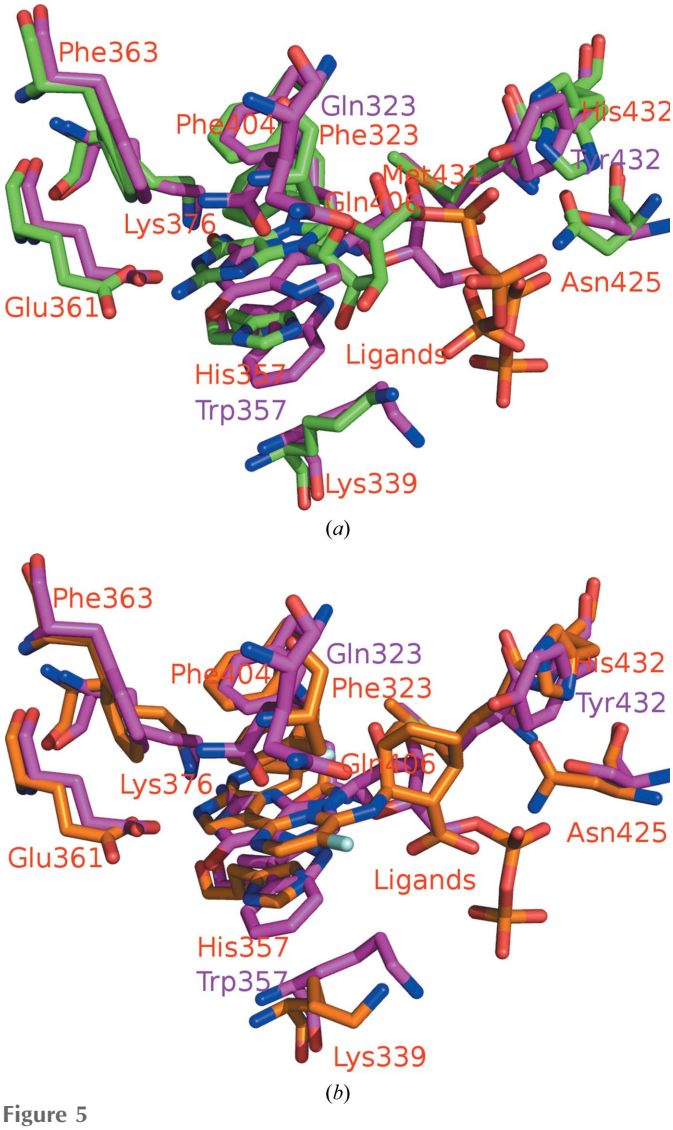

Figure 5
(*a*) Comparison of the GDP-bound cap-binding site in B/Jiangxi/BV/2006 PB2cap (PDB entry 4q46; magenta; Liu *et al.*, 2015) and the m^7GTP-bound cap-binding site in A/California/07/2009 PB2cap (green). Residues in B/Jiangxi/BV/2006 PB2cap are labeled in purple if they are different from those in A/California/07/2009 PB2cap. 'Ligands' indicates the locations of GDP and m^7GTP, respectively. (*b*) Comparison of the GDP-bound cap-binding site in B/Jiangxi/BV/2006 PB2cap (PDB entry 4q46; magenta) and the VX-787-bound cap-binding site in A/Victoria/3/1975 PB2cap (PDB entry 4p1u; orange; Clark *et al.*, 2014). Residues in B/Jiangxi/BV/2006 PB2cap are labeled in purple if they are different from those in A/California/07/2009 PB2cap. 'Ligands' indicates the locations of GDP and VX-787, respectively.

3.4. Differences from PB2cap of influenza B virus

VX-787 is not active against influenza B virus (Byrn *et al.*, 2015). Since influenza B virus is also a serious health threat, it is more desirable to have an inhibitor that is effective against both influenza A and B viruses. Comparison of the VX-787 complex structure with the GDP complex of influenza B PB2cap (Liu *et al.*, 2015) may suggest why VX-787 does not effectively inhibit influenza B viruses (Fig. 5*a*). The guanine moiety in PB2cap of influenza B virus B/Jiangxi/BV/2006 is rotated 180° relative to that in PB2cap of influenza A virus (Fig. 5*b*). As a result, the N atom at position 1 and the amino group linked to position 2 still form hydrogen bonds to the side chain of Glu361, but in a reversed orientation. The carbonyl at position 6 now forms a hydrogen bond to the side chain of Arg332 (Arg334 in influenza B virus) instead of that of Lys376. His357 is replaced by Trp, which makes more π–π stacking interactions with the guanine moiety. However, π–π stacking interactions on the other side are only retained for the side chain of Phe404. Phe323 is replaced by Gln, which can no longer provide π–π stacking. Moreover, His432 is replaced by Tyr, which has a bulkier side chain that provides steric hindrance to bicyclooctane. It seems that many of the favorable interactions between VX-787 and PB2cap of influenza A virus do not exist in PB2cap of influenza B virus, and more importantly some residues in PB2cap of influenza B virus

could potentially pose steric hindrance to VX-787, such as Tyr432. The characteristics of both cap-binding sites need to be considered simultaneously if one inhibitor is to be designed against both influenza A and B viruses.

3.5. Comparisons with human cap-binding proteins

Binding of an inhibitor to host cap-binding proteins needs to be avoided in order to design specific inhibitors of PB2cap. The structures of a cap-specific mRNA methyltransferase (Smietanski *et al.*, 2014) and the translation initiation factor eIF4E (Papadopoulos *et al.*, 2014) were used as examples (Fig. 6). In the methyltransferase, the carbonyl O atom in the guanine moiety forms a hydrogen bond to the main-chain amide N atom of Trp102 (Fig. 6*a*). The side chain of Glu103 forms two hydrogen bonds to the N atom at position 1 and the amino group linked to position 2, respectively. There are π–π stacking interactions made by Trp56 and Trp102 on each side of the guanine moiety. The methyl group linked to position 7 does not seem to be in a pocket, but is near the side chain of Trp166. There seems to be no direct interactions between the protein and the pyranose ring. On the other hand, strong interactions are present between the α- and β-phosphate groups and the side chain of Arg157, and between the β- and γ-phosphate groups and the side chain of Lys162.

In eIF4E, the side chain of Asp207 forms a hydrogen bond to the N atom at position 1 and that of Asn374 forms a hydrogen bond to the amino group linked to position 2 (Fig. 6*b*). There are no aromatic π–π stacking interactions with the guanine moiety, but the side chain of Glu373 shows an anion–aromatic stacking interaction with the guanine moiety. Again, there is no direction interaction with the pyranose ring. Charge or hydrogen-bond interactions are present between the β-phosphate group and the side chain of Asn439 and between the α- and γ-phosphate groups and the side chain of Arg218.

Overall, the interactions between the cap and the host proteins include those with the guanine and preferentially the phosphate groups. The binding site is not as deep as that in PB2cap. There is no interaction with the pyranose ring, which seems to serve only as a linker between the guanine moiety and the triphosphate.

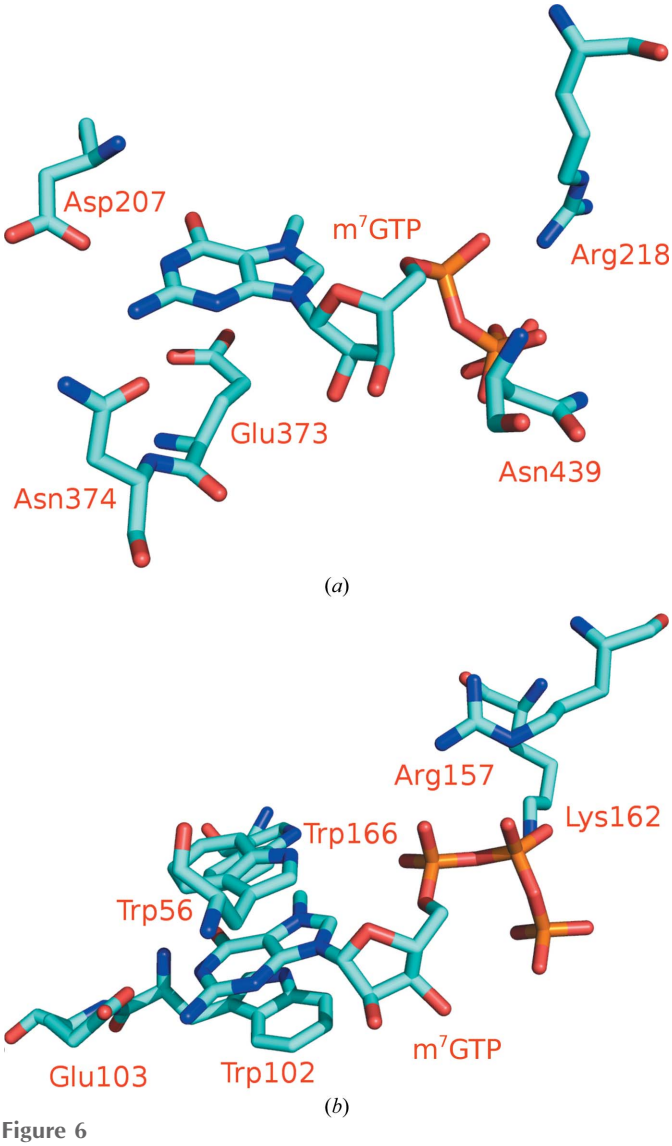

Figure 6
The cap-binding site (*a*) in the cap-specific mRNA methyltransferase bound to m^{7}GTP (PDB entry 4n49; Smietanski *et al.*, 2014) and (*b*) in the translation initiation factor eIF4E bound to m^{7}GTP (PDB entry 4tqb; Papodopolous *et al.*, 2014).

Acknowledgements

This work was supported in part by a grant from Beijing Natural Science Foundation (5152012). Data were collected on beamline BL17U of the Shanghai Synchrotron Radiation Facility and the Southeast Regional Collaborative Access Team (SER-CAT) 22-ID (or 22-BM) beamline at the Advanced Photon Source, Argonne National Laboratory (supporting institutions may be found at http://www.ser-cat.org/members.html). Use of the Advanced Photon Source was supported by the US Department of Energy, Office of Science, Office of Basic Energy Sciences under Contract No. W-31-109-Eng-38.

References

Byrn, R. A. *et al.* (2015). *Antimicrob. Agents Chemother.* **59**, 1569–1582.
Clark, M. P. *et al.* (2014). *J. Med. Chem.* **57**, 6668–6678.
Fraser, C. *et al.* (2009). *Science*, **324**, 1557–1561.
Guilligay, D., Tarendeau, F., Resa-Infante, P., Coloma, R., Crepin, T., Sehr, P., Lewis, J., Ruigrok, R. W. H., Ortin, J., Hart, D. J. & Cusack, S. (2008). *Nature Struct. Mol. Biol.* **15**, 500–506.
Klepser, M. E. (2014). *Drugs*, **74**, 1467–1479.
Liu, Y., Qin, K., Meng, G., Zhang, J., Zhou, J., Zhao, G., Luo, M. & Zheng, X. (2013). *J. Biol. Chem.* **288**, 11013–11023.
Liu, Y., Yang, Y., Fan, J., He, R., Luo, M. & Zheng, X. (2015). *J. Biol. Chem.* **290**, 9141–9149.
Nitsch-Osuch, A. & Brydak, L. B. (2014). *Acta Biochim. Pol.* **61**, 505–508.
Papadopoulos, E. *et al.* (2014). *Proc. Natl Acad. Sci. USA*, **111**, E3187–E3195.
Pautus, S., Sehr, P., Lewis, J., Fortuné, A., Wolkerstorfer, A., Szolar, O., Guilligay, D., Lunardi, T., Décout, J.-L. & Cusack, S. (2013). *J. Med. Chem.* **56**, 8915–8930.

Ruigrok, R. W. H., Crépin, T., Hart, D. J. & Cusack, S. (2010). *Curr. Opin. Struct. Biol.* **20**, 104–113.
Smietanski, M., Werner, M., Purta, E., Kaminska, K. H., Stepinski, J., Darzynkiewicz, E., Nowotny, M. & Bujnicki, J. M. (2014). *Nature Commun.* **5**, 3004.
Tarendeau, F., Boudet, J., Guilligay, D., Mas, P. J., Bougault, C. M., Boulo, S., Baudin, F., Ruigrok, R. W. H., Daigle, N., Ellenberg, J., Cusack, S., Simorre, J.-P. & Hart, D. J. (2007). *Nature Struct. Mol. Biol.* **14**, 229–233.
Tsurumura, T., Qiu, H., Yoshida, T., Tsumori, Y., Hatakeyama, D., Kuzuhara, T. & Tsuge, H. (2013). *PLoS One*, **8**, e82020.
Winn, M. D. *et al.* (2011). *Acta Cryst.* D**67**, 235–242.